Structure, Bonding, and Stability of a Catalytica Platinum(II) Catalyst: A Computational Study

Xin Xu,[†,‡] Jeremy Kua,[‡] Roy A. Periana,[§] and William A. Goddard III*,[‡]

Materials and Process Simulation Center (139-74), California Institute of Technology, Pasadena, California 91125, and Department of Chemistry, University of Southern California, Los Angeles, California 90089

Received March 21, 2002

Periana et al. [*Science* **1998**, *280*, 560] previously reported two catalysts for low-temperature methane activation to methanol: $PtCl_2(NH_3)_2$ and $PtCl_2$(bpym). It was shown that the ammine catalyst is much more active, but it decomposes rapidly in sulfuric acid to form a $PtCl_2$ precipitate, while the bpym system is long-lived. To have a basis for developing new catalysts that would not decompose, we undertook a study of the structure, bonding, and stability of the $PtCl_2(NH_3)_2$ and $PtCl_2$(bpym) catalysts, using quantum mechanics (QM) [density functional theory (DFT) at the B3LYP/LACVP**(+) level] including solvation in sulfuric acid via the Poisson−Boltzmann continuum approximation. Critical results include the following: (1) The influence of a trans ligand Y on the Pt−X bond follows the order Cl^- > NH_3 (bpym) > OSO_3H^- > □ (empty site). Thus the Pt−N bond length is longer (up to 0.04 Å) and the Pt−N bond is weaker (up to 18 kcal/mol) when trans to a Cl^- as compared to trans to OSO_3H^-. (2) The bpym ligand acts as both a σ-donor and a π-acceptor. As bpym is protonated, the Pt−N bond strength decreases (by up to 51 kcal/mol). Thus, ΔH(soln, 453 K) for $Pt(OSO_3H)_2$(bpym) (69.6) > $[Pt(OSO_3H)_2(bpymH)]^+$ (49.4) > $[Pt(OSO_3H)_2(bpymH_2)]^{2+}$ (18.7). (3) In sulfuric acid replacing the ammine ligands with bisulfate ligands is thermodynamically favorable [by ΔG(soln, 453 K) = −23 kcal/mol], whereas replacement of bpym with OSO_3H^- is unfavorable [by ΔG(soln, 453 K) = +16 kcal/mol]. (4) Replacement of chloride ligands with bisulfate ligands is thermodynamically unfavorable [by ΔG(soln, 453 K) = ∼7 kcal/mol for ammine and ∼12 kcal/mol for bpym]. (5) Protonation of $PtCl_2$(bpym) is thermodynamically favorable, leading to $[PtCl_2(bpymH)]^+$ as the stable species in sulfuric acid (by 8 kcal/mol). Thus we conclude that in hot concentrated sulfuric acid it is quite favorable for $PtCl_2(NH_3)_2$ to lose its ammine ligands to form $PtCl_2$, which in turn will dimerize and oligomerize, leading eventually to a $(PtCl_2)_n$ precipitate and catalyst death. We find that $PtCl_2$(bpym) is resistant to solvent attack, favoring retention of the bpym ligand in hot concentrated sulfuric acid. These results agree with experimental findings. The insights from these findings should help screen for stable new ligands in the design of new catalysts.

1. Introduction

Selective alkane oxidation by transition metal complexes in solution has been the focus of substantial effort since the 1970s.[1−20] However the low activity of alkanes and the typically higher activity of the desired products make this process a great challenge. Consequently, there are no commercial processes for the direct conversion of alkanes into more valuable products.

In 1998, Periana et al.[12] reported a significant breakthrough toward such processes. In well-dried sulfuric acid (80 mL at 102%), they found that 72% of 115 mmol

* To whom correspondence should be addressed. E-mail: wag@wag.caltech.edu.
† On sabbatical leave from Xiamen University, Xiamen 361005, China.
‡ California Institute of Technology.
§ University of Southern California.

(1) Arnstden, B. A.; Bergman, R. G.; Mobley, T. A.; Peterson, T. H. *Acc. Chem. Res.* **1995**, *28*, 154.
(2) Bromberg, S. E.; Yang, H.; Asplund, C. M.; Lian, T.; McNamara, K. B.; Kotz, K. T.; Yeston, J. S.; Wilkens, M.; Frei, H.; Bergman, R. G.; Harris, C. B. *Science* **1997**, *278*, 260.
(3) Davies, J. A., Watson, P. L., Liebman, J. L., Greenberg, A., Eds. *Selective Hydrocarbon Activation*; Wiley-VCH: New York, 1990.
(4) Hall, C.; Perutz, R. N. *Chem. Rev.* **1996**, *96*, 3125.
(5) Hill, C. L. *Activation and Functionalization of Alkanes*; Wiley-Interscience: New York, 1989.
(6) Sen, A. *Acc. Chem. Res.* **1988**, *21*, 421.
(7) Shilov, A. E.; Shul'pin, G. B. *Chem. Rev.* **1997**, *97*, 2879.
(8) Sommer, J.; Bukala, J. *Acc. Chem. Res.* **1993**, *26*, 370.
(9) Walktz, K. M.; Hartwig, J. F. *Science* **1997**, *277*, 211.
(10) Shilov, A. E. *Activation of Saturated Hydrocarbons by Transition Metal Complexes*; D. Riedel Publishing Co.: Dordrecht, The Netherlands, 1984.
(11) Periana, R. A.; Taube, D. J.; Evitt, E. R.; Loffler, D. G.; Wentrcek, P. R.; Voss, G.; Masuda, T. *Science* **1993**, *259*, 340.
(12) Periana, R. A.; Taube, D. J.; Gamble, S.; Taube, H.; Satoh, T.; Fujii, H. *Science* **1998**, *280*, 560.
(13) Hill, G. S.; Yap, G. P. A.; Puddephatt, R. J. *Organometallics* **1999**, *18*, 1408.
(14) Johansson, L.; Tilset, M. *J. Am. Chem. Soc.* **2001**, *123*, 739.
(15) Heiberg, H.; Johansson, L.; Gropen, O.; Ryan, O. B.; Swang, O.; Tilset, M. *J. Am. Chem. Soc.* **2000**, *122*, 10831.
(16) Mylvaganam, K.; Bacskay, G. B.; Hush, N. S. *J. Am. Chem. Soc.* **2000**, *122*, 2041.
(17) Heiberg, H.; Swang, O.; Ryan, O. B.; Gropen, O. *J. Phys. Chem.* **1999**, *A103*, 100004.
(18) Kua, J.; Xu, X.; Periana, R. A.; Goddard, W. A., III. *Organometallics* **2002**, *21*, 511.
(19) Mylavaganam, K.; Backsay, G. B.; Hush, N. S. *J. Am. Chem. Soc.* **1999**, *121*, 4633.
(20) Gilbert, T. M.; Hristov, I.; Ziegler. T. *Organometallics* **2001**, *20*, 1183.

10.1021/om0202165 CCC: $25.00
Publication on Web 04/05/2003

of CH_4 at 3.4 MPa was converted by 50 mmol of catalyst to products (a mixture of $CH_3OSO_3H + CH_3OH$) in 2.5 h at 220 °C. The initial catalyst is dichloro-(η^2-{2,2′-bipyrimidyl})platinum(II) complex, $PtCl_2$(bpym).

Higher initial activity than the bpym catalyst was reported for the ammine catalyst, $PtCl_2(NH_3)_2$. The extrapolated turnover frequency (TOF) of the ammine catalyst is on the order of 10^{-2} s^{-1}, an order of magnitude higher than that of the bpym catalyst (TOF $\approx 10^{-3}$ s^{-1}). The selectivity for the $PtCl_2(NH_3)_2$ catalyst to generate methyl bisulfate was found to be > 90%, higher than the 72% of the bpym catalyst. However the $PtCl_2(NH_3)_2$ catalyst soon degraded and $PtCl_2$ (solid) was precipitated after only several turnovers, halting the reaction ($\tau_{1/2} \approx 15$ min), whereas the bipyrimidine catalyst was stable and was still alive after over a thousand turnovers.

For a successful design of an effective catalyst, three factors must be taken into account: stability, activity, and selectivity.

An active catalyst must be selective and stable enough so that it will not degrade during a catalytic process; on the other hand, the stable catalyst must be active and selective enough to ensure a high yield of the desired product at low temperatures. For the Catalytica Pt(II) system[12] the primary issues are stability of the ligand−Pt complex in the hot, strongly acidic, and oxidizing environment and availability of open coordination sites for C−H activation.

To develop procedures to understand and predict issues related to catalyst stability, we considered the Catalytica Pt(II) catalysts $PtCl_2(NH_3)_2$ and $PtCl_2$(bpym) as prototypes and performed computational studies of the structure, bonding, and stability of these systems. These systems have been studied experimentally reasonably thoroughly, providing good validation for the theoretical methodologies. Our goal was to obtain useful criteria for judging the likely stability of new catalysts.

We report in this paper the thermodynamics for many possible stable species and intermediates of the ammine and bpym systems. In addition we explore their structures and the nature of the bonds.

Our calculations predict that the ammine complex should be short-lived, easily losing its ammine ligands in concentrated sulfuric acid. This leads to the formation of $PtCl_2$, which can then form dimers and trimers etc., and eventually aggregate to $(PtCl_2)_n$ precipitation, leading to catalyst death. This agrees with observation of short catalyst lifetime and observation of the precipitate.

On the other hand, we find that bipyrimidine acts as a "proton sink", allowing the protonated form of the ligand to remain bound to Pt in concentrated sulfuric acid. This agrees with the observed long lifetime and absence of precipitate.

The paper is arranged as follows. Section 2 summarizes the computational details. The optimized structures of possible stable species and intermediates of the ammine and bpym systems are presented in Section 3.1. In Section 3.2, we discuss the Pt−ligand bond energies. In Section 3.3, we address the thermodynamics of the possible ligand exchanges in the hot concentrated sulfuric acid. The mechanisms of precipitation are presented in Section 3.4. Concluding remarks are given in Section 4. Finally the accuracy of our methods is validated in the Appendix.

2. Computational Details

All quantum mechanical calculations were carried out using B3LYP of density functional theory,[21] which includes Becke's nonlocal gradient corrections[22] to the Slater local exchange functional[23] and some exact Hartree−Fock (HF) exchange, as well as the Vosko−Wilk−Nusair local correlation functional[24] and the Lee−Yang−Parr correlation functional.[25]

The core electrons of the Pt are treated with a nonlocal ECP using angular momentum projection operators to enforce the Pauli principle.[26,27] To do this, we use the Hay and Wadt[28] core−valence effective core potential (ECP), which treats explicitly the outer 18 electrons of Pt (5s, 5p, 5d, 6s, 6p). This basis set is denoted as LACVP** in the Jaguar QM software.[29,30] H, C, and N are treated at the level of 6-31G** (valence double-ζ plus polarization), while O, Cl, and S are treated by 6-31+G* with diffuse functions being added.

All calculations use the Poisson−Boltzmann (PB) continuum approximation to describe the effect of solvent.[31,32] In this approximation, the solvent accessible surface of the solute is calculated using van der Waals radii for the atoms and then rolling a sphere of radius R_{solv} over this surface to obtain a smooth surface. At each self-consistent field (SCF) step, we calculate the reaction field in the solvent due to the electrostatic field of the solute wave function using the experimental dielectric constant {$\epsilon = 98$ for 99% H_2SO_4[33] and radius $R_{solv} = 2.205$ Å[34]}. This reaction field is then included in the Fock operator (Kohn−Sham Hamiltonian) to calculate the orbitals of the DFT wave function of the solute. This calculation uses a numerical grid to describe the solvent region of space. For a fixed geometry, this process is continued until self-consistent. The total energy then includes the QM energy (which includes rearrangement effects due to the solvent) and the solute−solvent interactions. Ionic strength of the bulk solution is assumed to be zero in all our calculations.

All geometries are fully optimized in the gas phase. Vibrational frequencies are calculated analytically to ensure that each minimum is a true local minimum (only positive frequencies) and that each transition state has only a single imaginary frequency (negative eigenvalue of the Hessian). The DFT gas phase energy is corrected by the zero-point vibrations. In addition we use the vibrational frequencies to calculate the enthalpy and entropy as a function of temperature to obtain the total free energy. A single-point solvation calculation is

(21) Becke, A. D. *J. Chem. Phys.* **1993**, *98*, 5648.
(22) Becke, A. D. *Phys. Rev. A* **1988**, *38*, 3098.
(23) Slater, J. C. *Quantum Theory of Molecules and Solids*, Vol. 4: *The Self-Consistent Field for Molecules and Solids*; Mc-Graw Hill: New York, 1974.
(24) Vosko, S. H.; Wilk, L.; Nusair, M. *Can. J. Phys.* **1980**, *58*, 1200.
(25) Lee, C.; Yang, W.; Parr, R. G. *Phys. Rev. B* **1988**, *37*, 785.
(26) Goddard, W. A., III. *Phys. Rev.* **1968**, *174*, 659.
(27) Melius, C. F.; Olafson, B. O.; Goddard, W. A., III. *Chem. Phys. Lett.* **1974**, *28*, 457.
(28) Hay, P. J.; Wadt, W. R. *J. Phys. Chem.* **1985**, *82*, 299.
(29) *Jaguar 3.5*; Schrodinger, Inc.: Portland, OR, 1998.
(30) Greeley, B. H.; Russo, T. V.; Mainz, D. T.; Friesner, R. A.; Langlois, J.-M.; Goddard, W. A., III; Honig, B. *J. Am. Chem. Soc.* **1994**, *116*, 11875.
(31) Tannor, D. J.; Marten, B.; Murphy, R.; Friesner, R. A.; Sitkoff, D.; Nicholls, A.; Ringnalda, M.; Goddard, W. A., III; Honig, B. *J. Am. Chem. Soc.* **1994**, *116*, 11875.
(32) Marten, B.; Kim, K.; Cortis, C.; Friesner, R. A.; Murphy, R. B.; Ringnalda, M. N.; Sitkoff, D.; Honig, B. *J. Phys. Chem.* **1996**, *100*, 11775.
(33) Klassen, J. K.; Fiehrer, K. M.; Nathanson, G. M. *J. Phys. Chem. B* **1997**, *101*, 9098.
(34) Probe radius is calculated from $r^3 = 3m\Delta/4\pi\rho$ where r is the solvent probe radius in Å, m is the molecular mass obtained by dividing the molecular weight given in ref 27 in g/mol by Avogadro's number, 6.023×10^{23}, Δ is the packing density (assumed to be 0.5), and ρ is the density given in g/cm^3 at 20 °C obtained from ref 27.

Table 1. Geometric Parameters for $PtXY(NH_3)_2$, $PtXY(NH_3)$, and $PtX(NH_3)_2^+$ (X, Y = Cl, OSO_3H), Optimized at the B3LYP/LACVP(+) Level of Theory[a]**

complex	Pt−Cl	Pt−N	Pt−O	N−Pt−N	Cl−Pt−Cl	O−Pt−O	N−Pt−Cl	N−Pt−O	Cl−Pt−O
$PtCl_2(NH_3)_2$	2.347	2.123		98.5	95.5		83.0		
$PtCl(OSO_3H)(NH_3)_2$	2.349	2.087/2.116	2.058	99.5			84.5	84.0	92.0
$Pt(OSO_3H)_2(NH_3)_2$		2.088/2.090	2.058/2.061	99.4		93.2		79.9/87.5	
$PtCl_2(OSO_3H)(NH_3)^-$	2.351/2.368	2.084	2.111		96.0		88.5	86.7	89.1
$PtCl_2(OSO_3H)_2^{2-}$	2.337/2.347		2.138/2.167		91.4	89.7			87.0/91.9
$PtCl(NH_3)_2^+$	2.284	2.021/2.156		98.3			89.6/172.1		
$Pt(OSO_3H)(NH_3)_2^+$		2.027/2.122	1.996	95.9				93.4/170.5	
$PtCl_2(NH_3)$	2.278/2.297	2.114			105.8		83.8/170.4		
$PtCl(OSO_3H)(NH_3)$	2.277	2.097	2.013				162.6	81.7	115.7
$Pt(OSO_3H)_2(NH_3)$		2.094	1.996/2.022			94.0		90.0/175.9	
$PtCl_2(OSO_3H)^-$	2.310/2.316		2.066		97.7				96.0/166.0
$PtCl_2(\eta^2\text{-}OSO_3H)^-$	2.316		2.236		92.3	65.4			101.3
$PtCl_2$	2.227				113.2				
$PtCl(OSO_3H)$	2.223		1.912						127.8
$Pt(\eta^2\text{-}OSO_3H)_2$			2.090			68.8/111.2			

[a] All bond lengths are in angstroms, and all angles are in degrees. The optimized geometries of PtX_2, PtXY, PtX_2Y^-, and $PtX_2Y_2^{2-}$ are also included.

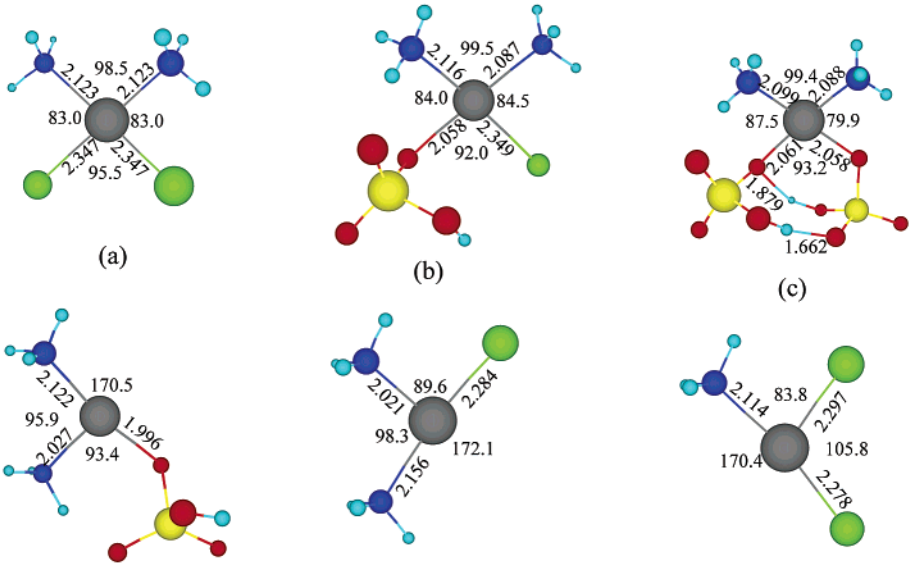

Figure 1. Optimized geometries for some key complexes of the ammine system: (a) $PtCl_2(NH_3)_2$; (b) $PtCl(OSO_3H)(NH_3)_2$; (c) $Pt(OSO_3H)_2(NH_3)_2$; (d) $[Pt(OSO_3H)(NH_3)_2]^+$; (e) $[PtCl(NH_3)_2]^+$; and (f) $PtCl_2(NH_3)$.

performed at each optimized gas phase geometry. Solvation (free) energies are added to the gas phase energies to obtain the solution phase (free) energies.

3. Results and Discussion

3.1. Geometries of Possible Stable Species and Intermediates. 3.1.1. Diammine Ligands. Table 1 summarizes the possible stable species and intermediates of the ammine system in hot concentrated sulfuric acid.

Starting from $PtCl_2(NH_3)_2$, chloride ligands may be replaced by bisulfate ligands, leading to the formation of $PtCl(OSO_3H)(NH_3)_2$ and $Pt(OSO_3H)_2(NH_3)_2$.

On the other hand, it is possible that ammine ligands would be replaced by bisulfate ligands, leading to the formation of $[PtCl_2(OSO_3H)(NH_3)]^-$and $[PtCl_2(OSO_3H)_2]^{2-}$. It was postulated[12] that one ligand of these square-planar Pt(II) complexes could be lost, resulting in a T-complex that would offer an open site for the activation of methane. Therefore we also optimized the geometry of possible T-complexes. The optimized geometric parameters of the ammine system are presented in Table 1. Figure 1 shows the geometries of some key complexes of the ammine system.

The coordination of one ligand to a metal ion influences the bonding between that metal ion and every other ligand. This influence has been intensively investigated and referred to as a trans-effect.[35,36] From the geometrical parameters shown in Table 1 and Figure 1, we note the following.

(1) The Pt−N bond length is 2.123 Å in $PtCl_2(NH_3)_2$. It decreases to 2.090 Å as two Cl ligands are replaced by two bisulfate ligands. In $PtCl(OSO_3H)(NH_3)_2$, the length of the Pt−N bond which is trans to the bisulfate ligand is 2.087 Å, shorter than that of the Pt−N bond (2.116 Å), which is trans to the chlorine ligand. These results indicate that the chlorine ligand is a better σ−donor and hence a better trans-influencing ligand than the bisulfate ligand.

(2) All Pt complexes basically preserve the square-planar arrangement. We find that X−Pt−X bond angles

(35) Cotton, F. A.; Wilkinson, G. *Advanced Inorganic Chemistry*; John Wiley: New York, 1988; pp 1299−1300.
(36) Atwood, J. D. *Inorganic and Organometallic Reaction Mechanisms*; Brooks/Cole Publishing Co.; Monterey, CA, 1985.

Table 2. Geometric Parameters for $PtXY(bpymH_n)^{n+}$ and $PtX(bpymH_n)^{n+1}$ (X, Y = Cl, OSO_3H, n = 0, 1, 2), Optimized at the B3LYP/LACVP(+) Level of Theory[a]**

complex	Pt−Cl	Pt−N	Pt−O	N−Pt−N	Cl−Pt−Cl	O−Pt−O	N−Pt−Cl	N−Pt−O	Cl−Pt−O
$PtCl_2(bpym)$	2.343	2.056		79.6	91.9		94.3		
$PtCl_2(bpymH)^+$	2.302/2.317	2.064/2.071		80.0	92.5		93.0/94.4		
$PtCl_2(bpymH_2)^{2+}$	2.291	2.061		78.5	90.5		95.5		
$PtCl(OSO_3H)(bpym)$	2.356	2.030/2.038	2.046	80.3			96.2	94.2	89.4
$PtCl(OSO_3H)(bpymH)^+$	2.305	2.051/2.059	2.037	80.5			95.0	93.7	90.8
$PtCl(OSO_3H)(bpymH_2)^{2+}$	2.286	2.035/2.051	2.020	79.1			96.3	94.8	89.7
$Pt(OSO_3H)_2(bpym)$		2.016/2.018	2.055/2.058	81.1		97.9		89.7/91.2	
$Pt(OSO_3H)_2(bpymH)^+$		2.036	2.012/2.026	81.4		99.8		89.1/89.6	
$Pt(OSO_3H)_2(bpymH_2)^{2+}$		2.016/2.046	1.977/1.998	79.8		100.1		89.0/91.1	
$PtCl(bpym)^+$	2.270	1.986/2.055		79.1			113.1/167.8		
$PtCl(bpymH)^{2+}$	2.235	1.998/2.099		79.5			111.1/169.4		
$PtCl(bpymH_2)^{3+}$	2.184	2.044		76.8			141.9		
$Pt(OSO_3H)(bpym)^+$		1.997/2.043	1.982	79.1				112.1/168.3	
$Pt(OSO_3H)(bpymH)^{2+}$		2.030/2.073	1.943	79.1				113.0/167.8	
$Pt(OSO_3H)(bpymH_2)^{3+}$		2.034/2.070	1.886	77.3				118.3/164.4	

[a] All bond lengths are in angstroms, and all angles are in degrees.

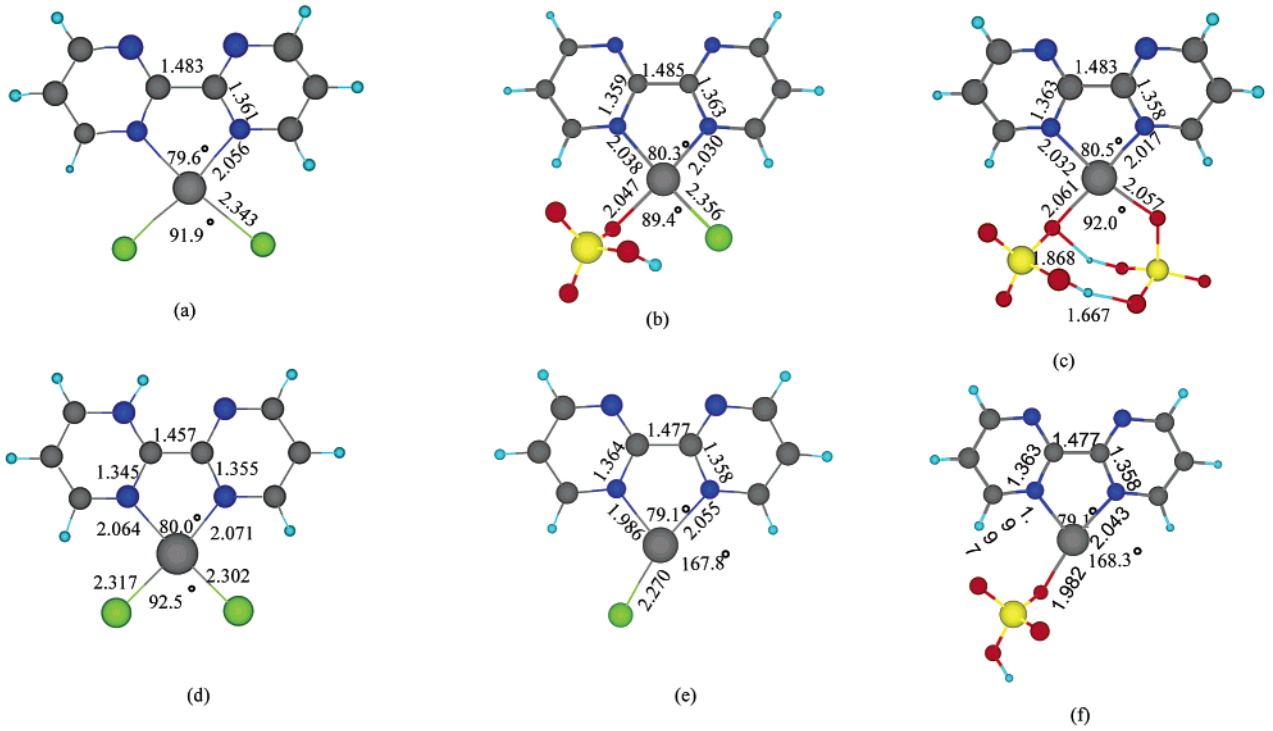

Figure 2. Optimized geometries for some key complexes of the bipyrimidine (bpym) system: (a) $PtCl_2(bpym)$; (b) $PtCl(OSO_3H)(bpym)$; (c) $Pt(OSO_3H)_2(bpym)$; (d) $[PtCl_2(bpymH)]^+$; (e) $[PtCl(bpym)]^+$; and (f) $[Pt(OSO_3H)(bpym)]^+$.

are generally larger than X−Pt−Y (X ≠ Y) bond angles. The largest bond angle is ∠N−Pt−N = 99.5° in $PtCl(OSO_3H)(NH_3)_2$, while the smallest bond angle is ∠N−Pt−O = 79.9° in $Pt(OSO_3H)_2(NH_3)_2$.

(3) Losing one ligand leads to the T-complex in Figure 1. The obtuse ∠X−Pt−Y angle ranges from 161.4° in $[PtCl(OSO_3H)_2]^-$ to 175.9° in $Pt(OSO_3H)_2(NH_3)$.

(4) In the T-complex, the length of the Pt−X bond trans to ligand Y is always longer than that of the Pt−X bond cis to ligand Y (trans to the empty site). Thus for $[PtCl(NH_3)_2]^+$ in Figure 1 the Pt−N bond trans to Cl^- (Pt−N = 2.156 Å) is longer than the Pt−N bond (2.021 Å) trans to the empty site. The only exception in Table 1 is $PtCl_2(NH_3)$ (see Figure 1), where the Pt−Cl bond length (2.278 Å) trans to NH_3 is shorter than that of the Pt−Cl bond (2.297 Å) trans to the empty site.

(5) In all Pt complexes shown in Table 1, the Pt−Cl bond lengths vary from 2.277 to 2.349 Å; the Pt−N bond distances vary from 2.021 to 2.156 Å, and the Pt−O vary from 1.996 to 2.167 Å. The average Pt−X bond length follows the trend Pt−Cl (2.316 Å) > Pt−N (2.097 Å) > Pt−O (2.056 Å).

3.1.2. Bipyrimidine Ligands. Table 2 summarizes the possible stable species and intermediates of the bpym system in hot concentrated sulfuric acid.

Starting from $PtCl_2(bpym)$, ligand substitutions by solvent lead to the formation of $PtCl(OSO_3H)(bpym)$, $Pt(OSO_3H)_2(bpym)$, etc.

Losing one chloride or bisulfate ligand could also be possible,[12] leading to the formation of $[PtCl(bpym)]^+$ or $[Pt(OSO_3H)(bpym)]^+$, etc.

In hot concentrated sulfuric acid, the backside nitrogen can be protonated, while still leaving two N's bound to the Pt(II) ion. Thus $PtXY(bpymH_n)^{n+}$ or $PtX(bpymH_n)^{(n+1)+}$ (X = Cl^-, OSO_3H^-, n = 0, 1, 2) are all possible stable species or intermediates of the bpym system. The

Table 3. Dissociation Energies of Pt−N Bonds, Calculated at the B3LYP/LACVP(+) Level of Theory[a]**

dissociation reaction	ΔE (g, 0K)	ΔH (g, 298K)	ΔG (g, 298K)	ΔH (s, 298K)	ΔG (s, 298K)	ΔH (s, 453K)	ΔG (s, 453K)
(1a) $PtCl_2(NH_3)_2 \rightarrow PtCl_2(NH_3) + NH_3$	43.8	41.5	30.4	34.7	23.6	34.4	17.9
(2a) $PtCl_2(NH_3) \rightarrow PtCl_2 + NH_3$	48.6	46.1	35.8	50.2	39.9	49.9	34.6
(3a) $PtCl(OSO_3H)(NH_3)_2 \rightarrow PtCl(OSO_3H)(NH_3) + NH_3$	52.9	50.4	38.8	52.7	41.1	52.4	35.1
(4a) $PtCl(OSO_3H)(NH_3) \rightarrow PtCl(OSO_3H) + NH_3$	54.1	51.4	40.6	48.1	37.2	47.8	31.6
(5a) $Pt(OSO_3H)_2(NH_3)_2 \rightarrow Pt(OSO_3H)_2(NH_3) + NH_3$	58.7	55.8	46.5	44.9	35.6	44.6	30.8
(6a) $Pt(OSO_3H)_2(NH_3) \rightarrow Pt(\eta^2\text{-}OSO_3H)_2 + NH_3$	21.7	19.2	6.6	41.4	28.7	41.3	22.2
(7a) $PtCl_2(bpym) \rightarrow PtCl_2 + bpym$	87.0	84.9	70.1	73.5	58.6	73.0	51.0
(8a) $PtCl_2(bpymH)^+ \rightarrow PtCl_2 + (bpymH)^+$	58.9	56.0	42.6	57.7	44.3	60.0	36.8
(9a) $PtCl_2(bpymH_2)^{2+} \rightarrow PtCl_2 + (bpymH_2)^{2+}$	26.6	25.9	11.6	39.1	24.9	38.5	17.6
(10a) $PtCl(OSO_3H)(bpym) \rightarrow PtCl(OSO_3H) + bpym$	98.7	96.4	79.3	86.1	69.0	85.7	60.2
(11a) $PtCl(OSO_3H)(bpymH)^+ \rightarrow PtCl(OSO_3H) + (bpymH)^+$	66.6	64.7	49.8	69.5	54.5	69.0	46.9
(12a) $PtCl(OSO_3H)(bpymH_2)^{2+} \rightarrow PtCl(OSO_3H) + (bpymH_2)^{2+}$	31.9	31.0	16.3	44.1	29.4	43.5	21.9
(13a) $Pt(OSO_3H)_2(bpym) \rightarrow Pt(\eta^2\text{-}OSO_3H)_2 + bpym$	72.0	69.4	52.0	69.8	52.4	69.6	43.5
(14a) $Pt(OSO_3H)_2(bpymH)^+ \rightarrow Pt(\eta^2\text{-}OSO_3H)_2 + (bpymH)^+$	30.0	28.6	12.6	49.7	33.8	49.4	25.5
(15a) $Pt(OSO_3H)_2(bpymH_2)^{2+} \rightarrow Pt(\eta^2\text{-}OSO_3H)_2 + (bpymH_2)^{2+}$	−8.2	−8.8	−23.3	19.3	4.9	18.7	−2.5

[a] All energies are in kcal/mol.

Table 4. Dissociation Energies of Pt−Cl and Pt−OSO_3H Bonds, Calculated at the B3LYP/LACVP(+) Level of Theory[a]**

dissociation reaction	ΔE (g, 0K)	ΔH (g, 298K)	ΔG (g, 298K)	ΔH (s, 298K)	ΔG (s, 298K)	ΔH (s, 453K)	ΔG (s, 453K)
(1b) $PtCl_2(NH_3)_2 \rightarrow PtCl(NH_3)_2^+ + Cl^-$	165.6	165.6	156.4	24.0	14.8	23.8	9.4
(2b) $PtCl(OSO_3H)(NH_3)_2 \rightarrow Pt(OSO_3H)(NH_3)_2^+ + Cl^-$	172.3	171.7	164.0	26.1	18.4	25.9	13.8
(3b) $PtCl(OSO_3H)(NH_3)_2 \rightarrow PtCl(NH_3)_2^+ + OSO_3H^-$	137.5	136.3	122.6	13.1	−0.6	12.6	−7.6
(4b) $Pt(OSO_3H)_2(NH_3)_2 \rightarrow Pt(OSO_3H)(NH_3)_2^+ + OSO_3H^-$	146.6	144.8	130.8	15.2	1.2	14.9	−6.1
(5b) $PtCl_2(bpym) \rightarrow PtCl(bpym)^+ + Cl^-$	155.4	155.1	146.1	36.1	27.1	36.0	21.8
(6b) $PtCl_2(bpymH)^+ \rightarrow PtCl(bpymH)^{2+} + Cl^-$	235.0	233.3	225.4	38.9	31.0	41.7	25.6
(7b) $PtCl_2(bpymH_2)^{2+} \rightarrow PtCl(bpymH_2)^{3+} + Cl^-$	317.9	317.5	307.8	50.8	41.1	50.6	35.4
(8b) $PtCl(OSO_3H)(bpym) \rightarrow PtCl(bpym)^+ + OSO_3H^-$	124.4	123.0	108.3	22.0	7.3	21.5	−0.2
(9b) $PtCl(OSO_3H)(bpymH)^+ \rightarrow PtCl(bpymH)^{2+} + OSO_3H^-$	200.1	198.6	185.6	24.0	11.1	23.5	4.5
(10b) $PtCl(OSO_3H)(bpymH_2)^{2+} \rightarrow PtCl(bpymH_2)^{3+} + OSO_3H^-$	280.6	279.1	265.5	29.1	15.5	28.5	8.5
(11b) $PtCl(OSO_3H)(bpym) \rightarrow Pt(OSO_3H)(bpym)^+ + Cl^-$	162.6	162.3	152.7	42.1	32.5	42.0	26.9
(12b) $PtCl(OSO_3H)(bpymH)^+ \rightarrow Pt(OSO_3H)(bpymH)^{2+} + Cl^-$	237.9	237.3	229.9	46.4	38.9	46.2	34.5
(13b) $PtCl(OSO_3H)(bpymH_2)^{2+} \rightarrow Pt(OSO_3H)(bpymH_2)^{3+} + Cl^-$	312.6	312.5	305.7	46.9	40.1	46.9	33.8
(14b) $Pt(OSO_3H)_2(bpym) \rightarrow Pt(OSO_3H)(bpym)^+ + OSO_3H^-$	136.9	135.2	118.4	29.5	12.7	29.3	4.1
(15b) $Pt(OSO_3H)_2(bpymH)^+ \rightarrow Pt(OSO_3H)(bpymH)^{2+} + OSO_3H^-$	202.6	200.9	185.5	30.3	15.0	30.0	7.1
(16b) $Pt(OSO_3H)_2(bpymH_2)^{2+} \rightarrow Pt(OSO_3H)(bpymH_2)^{3+} + OSO_3H^-$	273.4	272.5	259.0	25.8	12.4	25.5	3.3

[a] All energies are in kcal/mol.

optimized geometric parameters of the bpym system are listed in Table 2. Geometries of some key complexes of the bpym system are displayed in Figure 2. We note the following.

(1) The conclusions based on Table 1 of the ammine system generally apply to the bpym system, but because of the bidentate coordination nature of $(bpymH_n)^{n+}$ ligands, the N−Pt−N bond angles remain ∼80° for all Pt complexes shown in Table 2. The influence of a trans ligand Y on the Pt−X bond length also follows the same order: $Cl^- > NH_3$ (bpym) > OSO_3H^- > □ (empty site). Therefore the Pt−X bond is longer when it is trans to a stronger trans-influencing ligand Y. The average Pt−X bond length follows the trend Pt−Cl (2.320 Å) > Pt−N (2.094 Å) > Pt−O (2.060 Å).

(2) Bpym is generally considered as a π-acceptor, but we find that the trans-effects on geometry can also be interpreted in terms σ-donor character. As bpym is protonated, σ-basicity decreases and π-acidity increases. These two together contribute to the observed decreasing of Pt−Cl or Pt−O bond lengths in the series of $PtCl(OSO_3H)(bpym)$, $[PtCl(OSO_3H)(bpymH)]^+$, and $[PtCl(OSO_3H)(bpymH_2)]^{2+}$ (see Table 2).

3.2. Pt−Ligand Dissociation Energy. Table 3 and Table 4 present the dissociation energies of Pt−N, Pt−Cl, and Pt−OSO_3H bonds. We report ΔE (energy change), ΔH (enthalpy change), and ΔG (free energy change) at 0, 298, and 453 K in the gas phase and solution phase. Gas phase data indicate the intrinsic Pt−X bond strengths; solution phase data reflect the effect of solution. The 298 K data would be more relevant to the stability of the catalysts during the preparation, while the 453 K data provide a measure of bond strengths at the reaction situation. The discussion in this section focuses mainly on ΔE(g, 0 K), energy change of a dissociation reaction in gas phase at 0 K, and ΔH(s, 453 K), enthalpy change of a dissociation reaction in solution at 453 K.

3.2.1. Pt−N Bond Strength. Reactions 1a and 2a successively break the Pt−NH_3 bond in $PtCl_2(NH_3)_2$. Note that the second Pt−N bond is ∼15 kcal/mol *stronger* than the first Pt−N bond. As a chloride ligand is replaced by a bisulfate ligand, the Pt−N bond strength should increase since the chloride ligand is a better trans-influencing ligand than bisulfate. The gas phase numbers clearly show this tendency. For example, ΔE(g, 0 K) is 43.8 kcal/mol for reaction 1a, which increases to 52.9 kcal/mol in reaction 3a; ΔE(g, 0 K) is 48.6 kcal/mol for reaction 2a, which increases to 54.1 kcal/mol in reaciton 4a.

Solvation effect complicates the situation. Thus ΔH(s, 453 K) increases from 34.4 kcal/mol in reaction 1a to

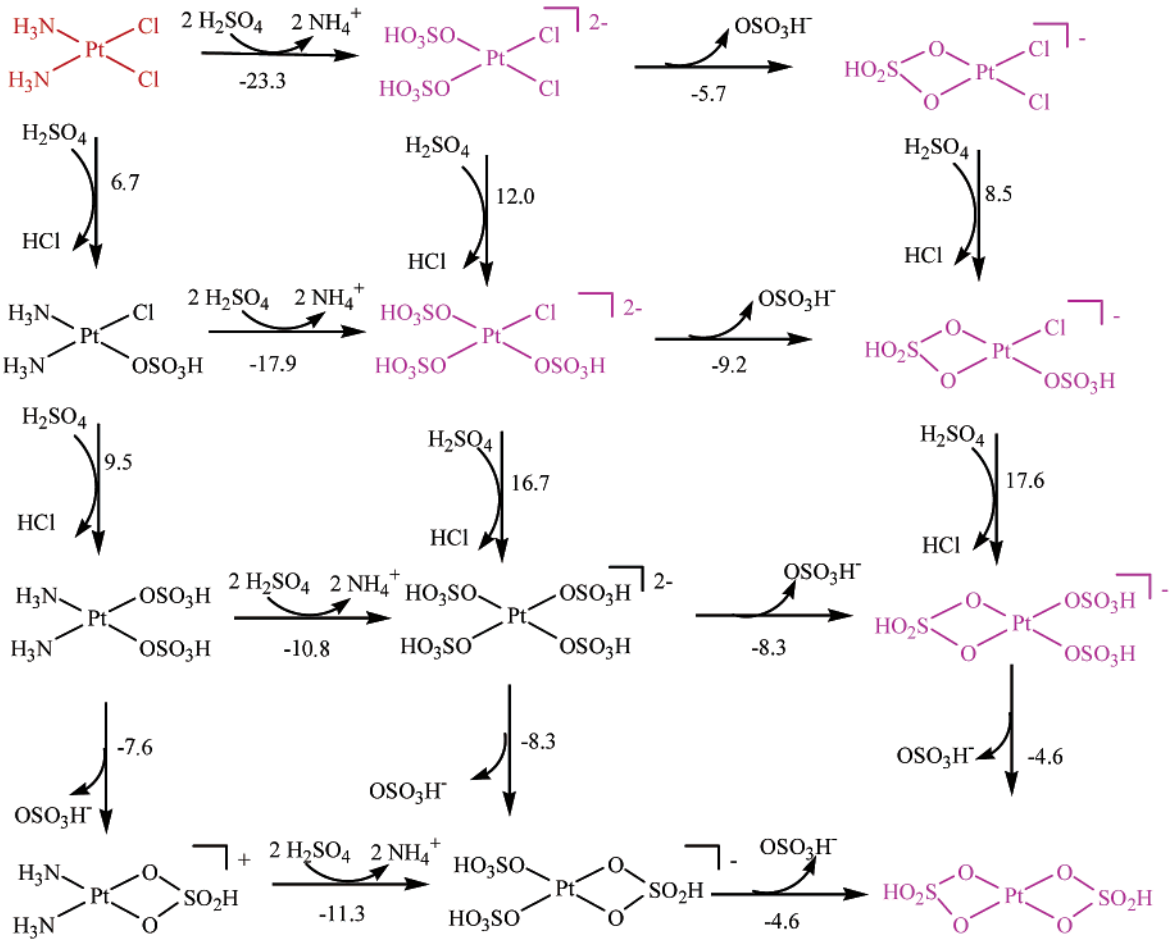

Figure 3. Ligand exchanges in the ammine system. ΔG(s, 453 K) is reported.

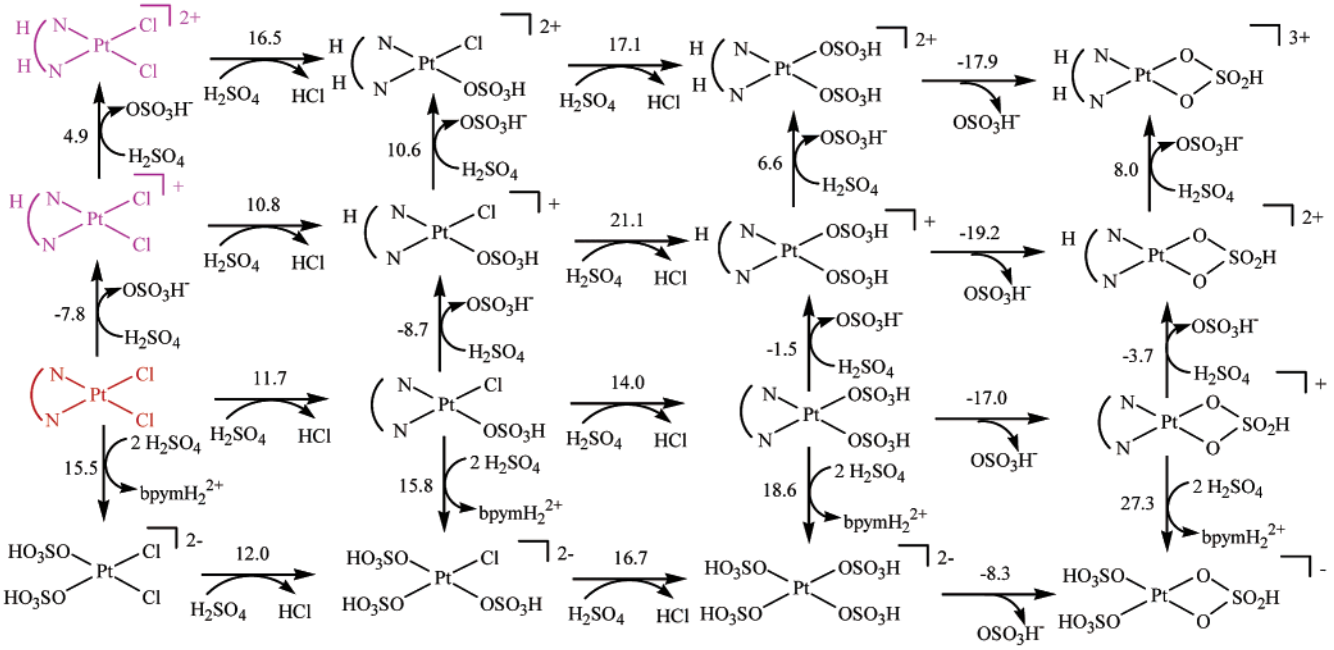

Figure 4. Ligand exchanges in the bipyrimidine (bpym) system. ΔG(s, 453 K) is reported.

52.4 kcal/mol in reaction 3a; ΔH(s, 453 K) decreases slightly from 49.9 kcal/mol in reaction 2a to 47.8 kcal/mol in reaction 4a.

The trans-effect would suggest that Pt−N bond strength follows the order $PtCl_2(NH_3)_2$ < $PtCl(OSO_3H)(NH_3)_2$ < $Pt(OSO_3H)_2(NH_3)_2$. This is true for the first Pt−NH_3 bond in the gas phase. But solvation effects lead to fluctuations.

We find that removing both NH_3 from $Pt(OSO_3H)_2(NH_3)_2$ is particularly easy. This is because the best

geometry of $Pt(OSO_3H)_2$ has the square-planar coordination structure, $Pt(\eta^2\text{-}OSO_3H)_2$ (see reaction 6a in Table 3).

Although the bpym ligand is generally considered as a π-acceptor,[12] we find that Pt−N dissociation reactions 7a−15a in Table 3, show clearly its role as a σ-donor. Thus as bpym is protonated, the Pt−N bond strength decreases, whereas we would expect that it would increase for a π-acceptor. For example, ΔE(g, 0 K) and ΔH(s, 453 K) follow the order ΔE(g, 0 K): $PtCl_2$(bpym) (87.0) > $[PtCl_2(bpymH)]^+$ (58.9) > $[PtCl_2(bpymH_2)]^{2+}$ (26.6); ΔH(s, 453 K): $PtCl_2$(bpym) (73.0) > $[PtCl_2(bpymH)]^+$ (60.0) > $[PtCl_2(bpymH_2)]^{2+}$ (38.5).

Summing the two Pt−NH_3 bonds in $PtXY(NH_3)_2$ and comparing with those for Pt−bpym, we find ΔE(g, 0 K): $PtCl_2(NH_3)_2$ (92.4) > $PtCl_2$(bpym) (87.0); $PtCl(OSO_3H)(NH_3)_2$ (107.1) > $PtCl(OSO_3H)$(bpym) (98.7); $Pt(OSO_3H)_2(NH_3)_2$ (80.4) > $Pt(OSO_3H)_2$(bpym) (72.0); ΔH(s, 453 K): $PtCl_2(NH_3)_2$ (84.3) > $PtCl_2$(bpym) (73.0); $PtCl(OSO_3H)(NH_3)_2$ (100.2) > $PtCl(OSO_3H)$(bpym) (85.7); $Pt(OSO_3H)_2(NH_3)_2$ (85.9) > $Pt(OSO_3H)_2$(bpym) (69.6). Thus the intrinsic Pt−N bond is stronger in the ammine complexes than in the bpym complexes.

3.2.2. Pt−OSO_3H and Pt−Cl Bond Strengths. From Table 4, we note the following.

(1) Solvation greatly stabilizes the ionic products. Thus, for example for reaction 1b, ΔE(g, 0 K) is 165.6 kcal/mol, ΔH(s, 453 K) is 23.8 kcal/mol.

(2) It is easier to dissociate a Pt−OSO_3H bond than to dissociate a Pt−Cl bond, making ΔH(s, 453 K) for reaction 3b ~11 kcal/mol smaller than for reaction 1b.

(3) The bisulfate ligand is a weaker cis-influencing ligand than the chloride ligand. For example, the Pt−Cl bond in $PtCl(OSO_3H)(NH_3)_2$ is slightly stronger (~2 kcal/mol) than in $PtCl_2(NH_3)_2$.

(4) Since bpym is a weaker σ-donor than NH_3, bpym is a weaker trans-influencing ligand than NH_3. Thus it is easier to dissociate a Pt−Cl bond in $PtCl_2(NH_3)_2$ (ΔH(s, 453 K) = 23.8 kcal/mol in reaction 1b) than to dissociate a Pt−Cl bond in $PtCl_2$(bpym) (ΔH(s, 453 K) = 36.0 kcal/mol in reaction 5b).

(5) As bpym is protonated, the σ-basicity of bpym is decreased. Thus we see that the Pt−Cl bond strength is increased in the series from $PtCl_2$(bpym) (ΔH(s, 453 K) = 36.0 kcal/mol) to $[PtCl_2(bpymH)]^+$ (41.7 kcal/mol) to $[PtCl_2(bpymH_2)]^{2+}$ (50.6 kcal/mol).

(6) For reactions 14b, 15b, and 16b, we have the Pt−OSO_3H bond dissociation energies in the gas phase (ΔE(g, 0 K)) in the order $Pt(OSO_3H)_2$(bpym) (136.9) < $[Pt(OSO_3H)_2(bpymH)]^+$ (202.6) < $[Pt(OSO_3H)_2(bpymH_2)]^{2+}$ (273.4).

In the solution phase (ΔH(s, 453 K)), however, we have $[Pt(OSO_3H)_2(bpymH_2)]^{2+}$ (25.5) < $Pt(OSO_3H)_2$(bpym) (29.3) < $[Pt(OSO_3H)_2(bpymH)]^+$ (30.0).

Solvation effect smooths the difference and/or even reverses the trend.

3.3. Thermodynamics of Ligand Exchanges. 3.3.1. Diammine Ligands. Figure 3 and Figure 4 show the thermodynamics of ligand exchanges. The numbers reported are free energy changes in solution at 453 K, ΔG(s, 453 K). Note that we do not correct the free energy for concentration differentials among reacting species to obtain the chemical potential. Such concentration corrections can be significant since the solvent (sulfuric acid) is present in much higher concentration than the other species in solution.

We find that replacement of ammine ligands with bisulfate ligands is thermodynamically favorable, while replacement of chloride ligands with bisulfate ligands is thermodynamically unfavorable. Thus

$$PtCl_2(NH_3)_2 + 2\ H_2SO_4 \rightarrow 2\ NH_4^+ + [PtCl_2(OSO_3H)_2]^{2-} \quad (3.3.1)$$

$$\Delta G\ (\text{s, 453 K}) = -23.3\ \text{kcal/mol}$$

$$PtCl_2(NH_3)_2 + 2\ H_2SO_4 \rightarrow Pt(OSO_3H)_2(NH_3)_2 + 2\ HCl \quad (3.3.2)$$

$$\Delta G(\text{s, 453 K}) = 16.2\ \text{kcal/mol}$$

Reaction 3.3.2 has been studied computationally by K. Mylvaganam et al.[19] Their calculations did not include polarization functions or diffuse functions, and in addition they used pseudopotentials for C, N, O, S, and Cl. Another difference is that their solvation energy was calculated using the isodensity polarized continuum model, whose results for ions are unreliable, with errors often greater than 20 kcal/mol, especially in the case of negative ions, for which the isodensity surfaces are markedly too far from the solute molecules.[37] They obtained ΔG(s, 473 K) = −31.9 kcal/mol for reaction 3.3.2, which is significantly different from the +16.2 kcal/mol we get. Thus they predict that chloride ligands can be favorably replaced by bisulfate ligands. The Appendix shows the procedure we used to establish the accuracy of our methods.

3.3.2. Bipyrimidine Ligands. We find protonation of $PtCl_2$(bpym) is a thermodynamically favorable process. Thus

$$PtCl_2(bpym) + H_2SO_4 \rightarrow [PtCl_2(bpymH)]^+ + [HSO_4]^- \quad (3.3.3)$$

$$\Delta G(\text{s, 453 K}) = -7.8\ \text{kcal/mol}$$

$$PtCl_2(bpym) + 2\ H_2SO_4 \rightarrow [PtCl_2(bpymH_2)]^{2+} + 2\ [HSO_4]^- \quad (3.3.4)$$

$$\Delta G(\text{s, 453 K}) = -2.9\ \text{kcal/mol}$$

However, we find replacement of bpym by bisulfate ligands is thermodynamically unfavorable.

$$PtCl_2(bpym) + 2\ H_2SO_4 \rightarrow [PtCl_2(OSO_3H)_2]^{2-} + [bpymH_2]^{2+} \quad (3.3.5)$$

$$\Delta G(\text{s, 453 K}) = 15.5\ \text{kcal/mol}$$

This is in sharp contrast to reaction 3.3.1, even though the intrinsic Pt−N is stronger in $PtCl_2(NH_3)_2$ than that in $PtCl_2$(bpym) (see Section 3.2).

Just as for $PtCl_2(NH_3)_2$, we find that replacement of a chloride ligand by a bisulfate ligand is thermodynamically unfavorable. Thus,

$$PtCl_2(bpym) + H_2SO_4 \rightarrow PtCl(OSO_3H)(bpym) + HCl \quad (3.3.6)$$

$$\Delta G(\text{s, 453 k}) = 11.7\ \text{kcal/mol}$$

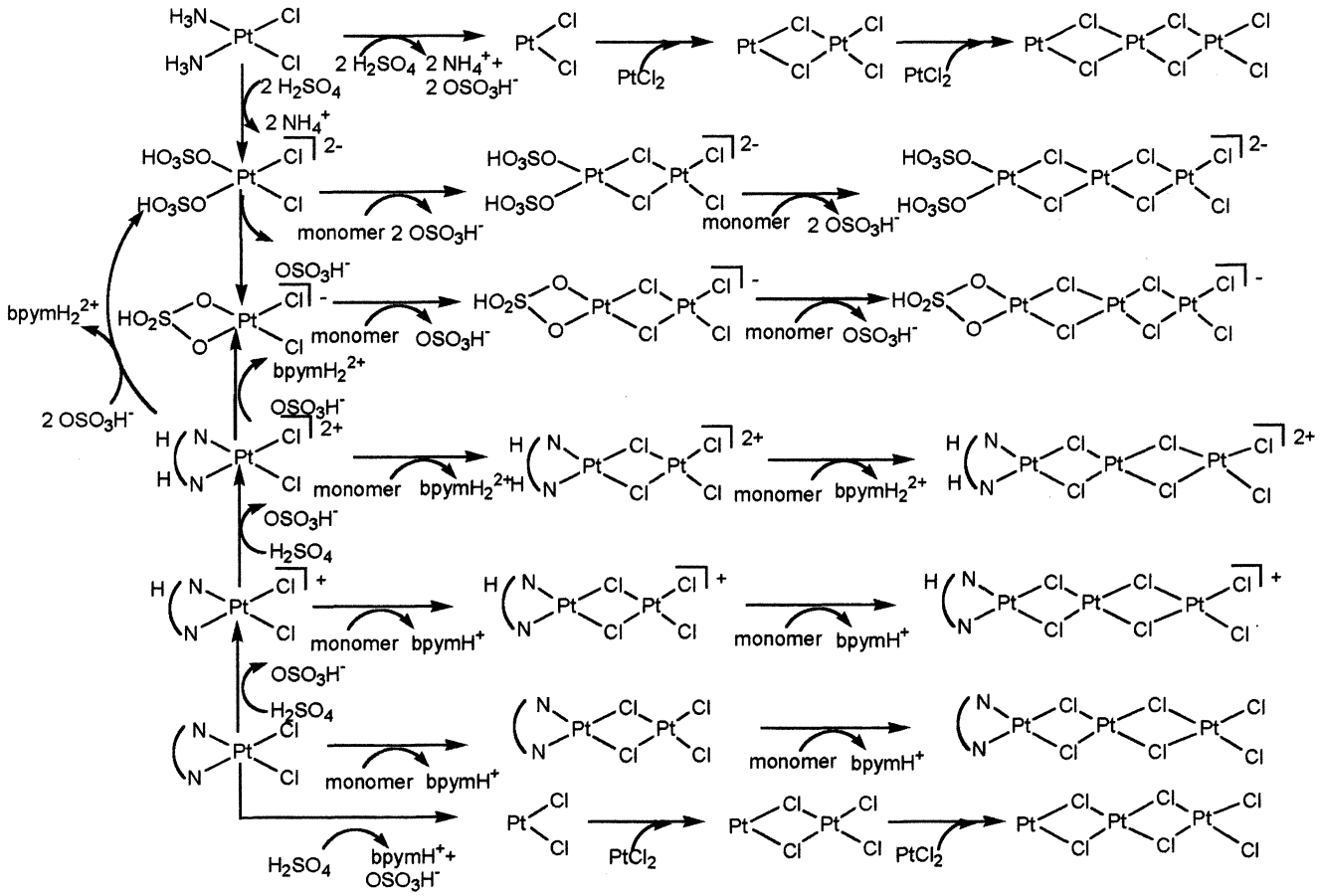

Figure 5. Possible mechanisms of precipitation.

This is reasonable. Comparing ΔG(s, 453 K) in eqs 5b and 8b indicates that dissociation of the Pt−Cl bond is 22.0 kcal/mol more endothermic than that of the Pt−OSO_3H bond, because the Pt−Cl bond is stronger than the Pt−OSO_3H bond. Since Cl^- is a better trans-influencing ligand than OSO_3H^-, the Pt−N bond in $PtCl(OSO_3H)$(bpym) is 9.2 kcal/mol more stable than that in $PtCl_2$(bpym) (see ΔG(s, 453 K) of eqs 7a and 10a in Table 3). The net effect is that replacing one Cl^- in $PtCl_2$(bpym) with OSO_3H^- should be uphill by 22.0 − 9.2 = 12.8 kcal/mol. This number agrees very well with the ΔG(s, 453 K) = 11.7 kcal/mol we get from reaction 3.3.6. In fact, similar arguments can be used to explain the endothermicity of reaction 3.3.2.

Our conclusion from reactions 3.3.3 and 3.3.4 is that $PtCl_2$(bpym) favors having one or two H on the bpym. This differs from the conclusions of Gilbert et al.,[20] who used the PW91 functional in the ADF DFT code combined with COSMOS solvation model to study

$$[PtCl(bpym)]^+ + H_2SO_4 \rightarrow [PtCl(bpymH)]^{2+} + [HSO_4]^- \quad (3.3.7)$$

$$[PtCl(bpym)]^+ + 2\ H_2SO_4 \rightarrow [PtCl\ (bpymH_2)]^{3+} + 2\ [HSO_4]^- \quad (3.3.8)$$

They assumed that one chloride ligand is lost and considered $[PtCl(bpym)]^+$ as the starting catalyst. They found both reactions 3.3.7 and 3.3.8 to be endothermic, with reaction energies of 6.9 and 34.2 kcal/mol, respectively, although they do not state clearly whether these numbers correspond to ΔE, ΔH, or ΔG or what temperature was used. They concluded that the peripheral bpym nitrogen atoms are not protonated in the Catalytica catalyst. We believe that it is important to take $PtCl_2$(bpym) as the starting catalyst. And we refer to our previous work[18] for details of the C−H activation in the protonated $PtCl_2$(bpym) and $PtCl(OSO_3H)$(bpym) catalytic systems.

3.4. Stability of the Ammine and the Bpym Systems. Periana et al. found that the ammine catalyst decomposes at 180 °C with a half-life of ∼15 min, leading to the irreversible protonation of the NH_3 ligands to generate insoluble $PtCl_2$ and NH_4HSO_4.[12]

We find

$$PtCl_2(NH_3)_2 + 2\ H_2SO_4 \rightarrow PtCl_2 + 2\ [NH_4]^+ + 2\ [HSO_4]^- \quad (3.4.1)$$

$$\Delta G(\text{s, 453 K}) = -24.1 \text{ kcal/mol}$$

$$2\ PtCl_2 \rightarrow (PtCl_2)_2 \quad (3.4.2)$$

$$\Delta G(\text{s, 453 K}) = -17.2 \text{ kcal/mol}$$

$$(PtCl_2)_2 + PtCl_2 \rightarrow (PtCl_2)_3 \quad (3.4.3)$$

$$\Delta G(\text{s, 453 K}) = -25.6 \text{ kcal/mol}$$

$$6\ PtCl_2 \rightarrow (PtCl_2)_6 \quad (3.4.4)$$

$$\Delta G(\text{s, 453 K}) = -104.5 \text{ kcal/mol}$$

Thus our calculations show that $PtCl_2(NH_3)_2$ will lose its ammine ligands in hot concentrated sulfuric acid,

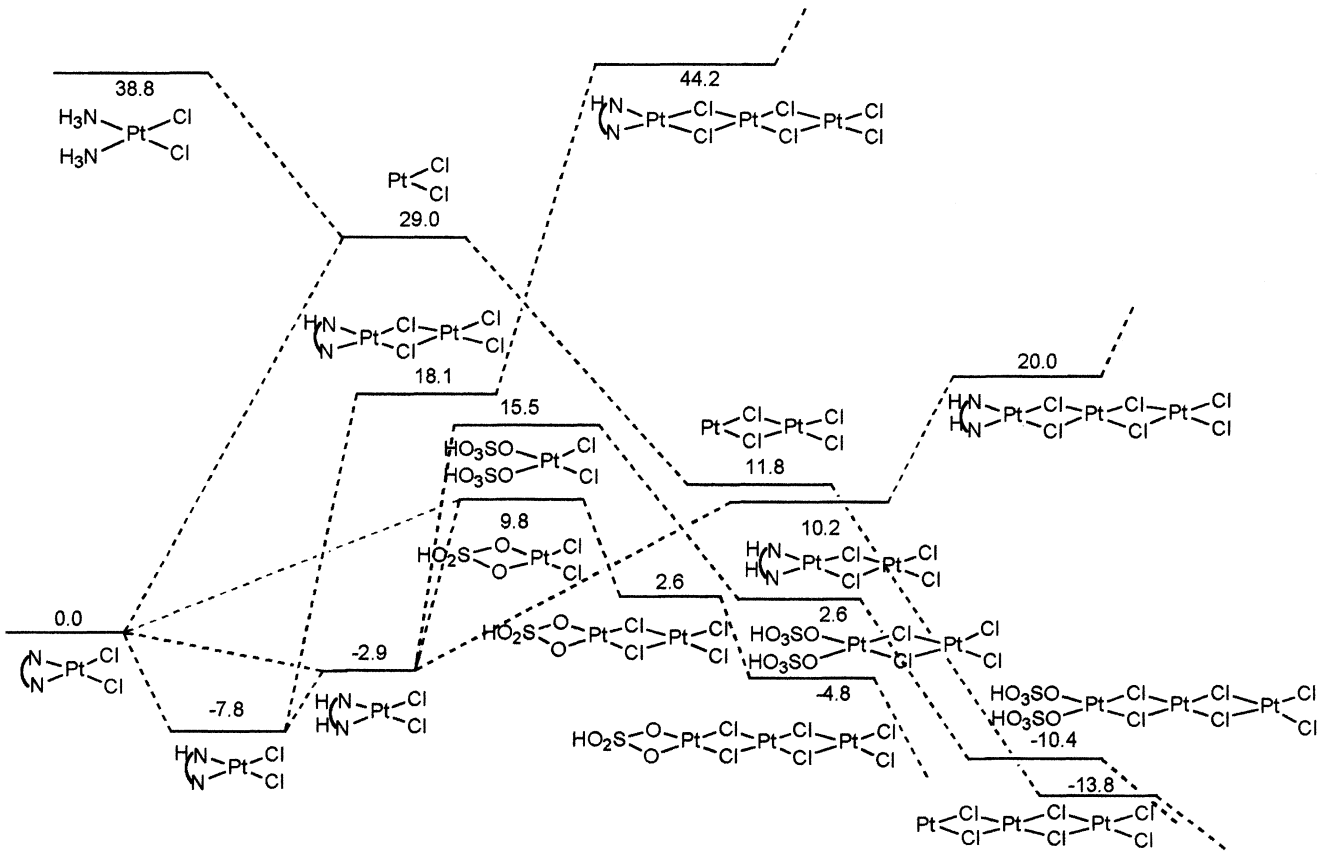

Figure 6. Energetics, ΔG(s, 453 K), of reactions shown in Figure 5.

and $PtCl_2$ will dimerize, trimerize, etc., leading to $(PtCl_2)_n$ precipitation, in agreement with the experimental findings.

Periana et al. found that a 50 mM solution of $PtCl_2$(bpym) in 20% *oleum*, even after 200 °C for 50 h, showed no evidence of ligand attack as monitored by nuclear magnetic resonance (NMR) spectroscopy. The $PtCl_2$(bpym) solution remained homogeneous, and no insoluble $(PtCl_2)_n$ formation or decomposition to Pt metal was observed.[12]

We find

$$PtCl_2(bpym) + H_2SO_4 \rightarrow PtCl_2 + [bpymH]^+ + [HSO_4]^- \quad (3.4.5)$$

$$\Delta G(\text{s, 453 K}) = 29.1 \text{ kcal/mol}$$

$$PtCl_2(bpym) + 2\ H_2SO_4 \rightarrow PtCl_2 + [bpymH_2]^{2+} + 2\ [HSO_4]^- \quad (3.4.6)$$

$$\Delta G(\text{s, 453 K}) = 14.7 \text{ kcal/mol}$$

Thus our calculations show that $PtCl_2$(bpym) is indeed resistant to solvent attack, favorably retaining the bpym ligand in hot concentrated sulfuric acid.

Recall from Figure 4 that the ammine ligands would be eventually replaced by the bisulfate ligands, while bpym tends to be protonated. We calculate the relative energetics for dimerization and trimerization of $[PtCl_2(OSO_3H)_2]^{2-}$, $[PtCl_2(\eta^2\text{-}OSO_3H)]^-$, $[PtCl_2(bpymH)]^+$, and $[PtCl_2(bpymH_2)]^{2+}$. We find that both bisulfate forms favorably form dimers and trimers. Thus, for example,

$$2\ [Pt(OSO_3H)_2Cl_2]^{2-} \rightarrow [(OSO_3H)_2Pt_2Cl_4]^{2-} + 2\ [OSO_3H]^- \quad (3.4.7)$$

$$\Delta G(\text{s, 453 K}) = -12.9 \text{ kcal/mol}$$

$$[(OSO_3H)_2Pt_2Cl_4]^{2-} + [Pt(OSO_3H)_2Cl_2]^{2-} \rightarrow [(OSO_3H)_2Pt_3Cl_6]^{2-} + 2\ [OSO_3H]^- \quad (3.4.8)$$

$$\Delta G(\text{s, 453 K}) = -13.0 \text{ kcal/mol}$$

On the other hand, it is unfavorable for the bipyrimidine catalyst to form dimers and trimers. For example,

$$2\ [PtCl_2(bpymH)]^+ \rightarrow [(bpymH)Pt_2Cl_4]^+ + [bpymH]^+ \quad (3.4.9)$$

$$\Delta G(\text{s, 453 K}) = 25.9 \text{ kcal/mol}$$

$$[(bpymH)Pt_2Cl_4]^+ + [PtCl_2(bpymH)]^+ \rightarrow [(bpymH)Pt_3Cl_6]^+ + [bpymH]^+ \quad (3.4.10)$$

$$\Delta G(\text{s, 453 K}) = 26.1 \text{ kcal/mol}$$

The reactions and related energetics are summarized in Figure 5 and Figure 6. In Figure 6, we take $PtCl_2$(bpym) as the reference state. To compare the stability of $PtCl_2(NH_3)_2$ to that of $PtCl_2$(bpym), we use the common decomposition product $PtCl_2$ as the reference. Here we see the reaction 3.4.5 from $PtCl_2$(bpym) to $PtCl_2$

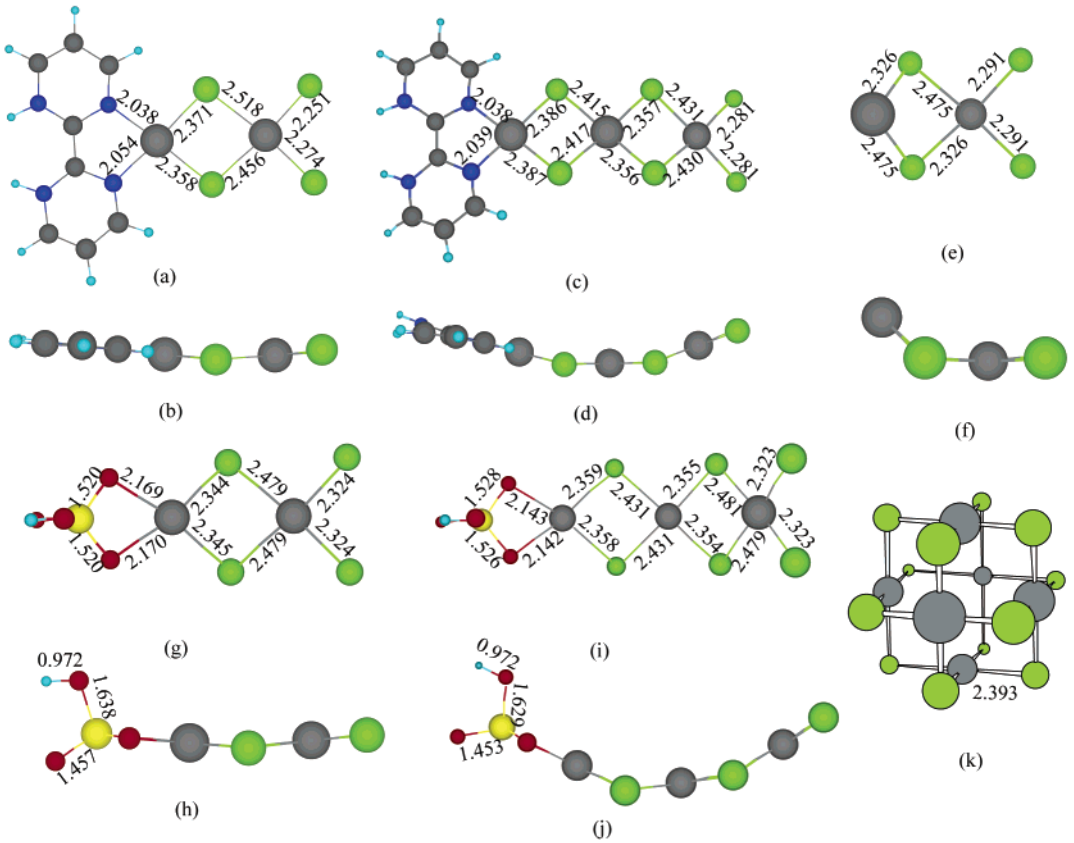

Figure 7. Optimized geometries of Pt(II) dimers, trimers, and hexamer: (a and b) $[Pt_2Cl_4(bpymH_2)]^{2+}$; (c and d) $[Pt_3Cl_6(bpymH_2)]^{2+}$; (e and f) $(PtCl_2)_2$; (g and h) $[Pt_2Cl_4(\eta^2\text{-}OSO_3H)]^-$; (i and j) $[Pt_3Cl_6(\eta^2\text{-}OSO_3H)]^-$; and (k) $(PtCl_2)_6$.

is *uphill* by 14.7 kcal/mol, whereas the reaction 3.4.1 from $PtCl_2(NH_3)_2$ to $PtCl_2$ is *downhill* by 24.1 kcal/mol. Thus $PtCl_2(NH_3)_2$ is 38.8 kcal/mol uphill with respect to $PtCl_2$(bpym).

Some of the optimized geometries of Pt(II) dimers, trimers, and hexamers are shown in Figure 7. Although each Pt(II) keeps a local square-planar geometry, it is interesting that the Pt(II) dimers and trimers adopt a bowl structure. The totally planar geometry is *not* a local minimum.

Experimentally, treatment of insoluble $(PtCl_2)_n$ with 1 equiv of bpym (50 mM) in concentrated H_2SO_4 at 150 °C leads to complete dissolution of $(PtCl_2)_n$ and formation of a homogeneous solution of $PtCl_2$(bpym).[12]

We find

$$PtCl_2 + [bpymH_2]^{2+} \rightarrow [PtCl_2(bpymH_2)]^{2+} \quad (3.4.11)$$

$$\Delta G(\text{s, 453 K}) = -17.6 \text{ kcal/mol}$$

$$(PtCl_2)_2 + 2\,[bpymH_2]^{2+} \rightarrow 2\,[PtCl_2(bpymH_2)]^{2+} \quad (3.4.12)$$

$$\Delta G(\text{s, 453 K}) = -18.0 \text{ kcal/mol}$$

$$(PtCl_2)_3 + 3\,[bpymH_2]^{2+} \rightarrow 3\,[PtCl_2(bpymH_2)]^{2+} \quad (3.4.13)$$

$$\Delta G(\text{s, 453 K}) = -27.2 \text{ kcal/mol}$$

$$(PtCl_2)_6 + 6\,[bpymH_2]^{2+} \rightarrow 6\,[PtCl_2(bpymH_2)]^{2+} \quad (3.4.14)$$

$$\Delta G(\text{s, 453 K}) = -1.1 \text{ kcal/mol}$$

By comparison, we find

$$PtCl_2 + 2\,[HSO_4]^- \rightarrow [PtCl_2(OSO_3H)_2]^{2-} \quad (3.4.15)$$

$$\Delta G(\text{s, 453 K}) = 0.8 \text{ kcal/mol}$$

$$(PtCl_2)_2 + 4\,[HSO_4]^- \rightarrow 2\,[PtCl_2(OSO_3H)_2]^{2-} \quad (3.4.16)$$

$$\Delta G(\text{s, 453 K}) = 18.8 \text{ kcal/mol}$$

$$(PtCl_2)_3 + 6\,[HSO_4]^- \rightarrow 3\,[PtCl_2(OSO_3H)_2]^{2-} \quad (3.4.17)$$

$$\Delta G(\text{s, 453 K}) = 27.9 \text{ kcal/mol}$$

$$(PtCl_2)_6 + 12\,[HSO_4]^- \rightarrow 6\,[PtCl_2(OSO_3H)_2]^{2-} \quad (3.4.18)$$

$$\Delta G(\text{s, 453 K}) = 109.2 \text{ kcal/mol}$$

These are in line with the experimental finding that treatment of $(PtCl_2)_n$ in hot concentrated H_2SO_4 with >100 equiv of NH_3 does not lead to $(PtCl_2)_n$ dissolution,[12] as NH_3 goes into H_2SO_4 as NH_4^+ and thus loses its coordination capability.

We also find

$$Pt(0) + bpym + 4\,H_2SO_4 \rightarrow [Pt(OSO_3H)_2(bpymH)]^+ + SO_2 + 2\,H_2O + [OSO_3H]^- \quad (3.4.19)$$

$$\Delta G(\text{s, 453 K}) = -108.4 \text{ kcal/mol}$$

$$\mathrm{Pt\ (0) + 3\ H_2SO_4 \rightarrow}$$
$$\mathrm{Pt(\eta^2\text{-}OSO_3H)_2 + SO_2 + 2\ H_2O} \quad (3.4.20)$$
$$\Delta G(\mathrm{s,\ 453\ K}) = -62.1\ \mathrm{kcal/mol}$$

Taking into account the experimental sublimation energy, 114.0 kcal/mol,[38] of bulk Pt metal, we may conclude that hot concentrated H_2SO_4 in the presence of bpym can dissolve Pt metal, so that the bpym system is not subject to the Pt black formation, a notorious problem well-documented in the Wacker system[39] as well as the Shilov Pt system for alkane oxidation.[10] In fact, it is found experimentally that a solution of bpym (20 mM) in hot, 96% H_2SO_4 leads to the oxidative dissolution of Pt metal (in the form of Pt black) to produce a homogeneous solution of $Pt(OSO_3H)_2(bpym)$.[12] Control experiments showed that no such dissolution occurs in the absence of the bpym ligand.[12] Thus our calculations demonstrate the effectiveness of the bpym ligand for maintaining the homogeneity of Pt cations in strong acids under strongly oxidizing, high-temperature conditions, in full agreement with the experimental findings.

4. Concluding Remarks

We performed computational studies of the structure, bonding, and stability of the Catalytica Pt(II) catalysts. All calculations were carried out at the B3LYP/LACVP**-(+) level, including the Poisson−Boltzmann continuum approximation to describe solvation effects.

Our conclusion is that to design a ligand suitable for a catalyst to be stable in concentrated sulfuric acid, one should ensure that the ligand in its optimum state of protonation in the sulfuric acid solvent still has unprotonated sites suitable for binding strongly to the metal center. The bipyrimidine ligand (singly or doubly protonated in solution) still has the two N centers available to bind to the complex. On the other hand for ammines and primary amines, it is quite favorable to form free RNH_3^+ in sulfuric acid solution, leading to loss of the ligands and eventually to precipitation of $PtCl_2$ and catalyst death. We expect that the most favorable ligands should have at least three N sites including two nitrogens in the right positions to form a bidentate ligand to the Pt complex plus at least one N for a proton.

Our results can be summarized as follows.

(1) The influence of a trans ligand Y on the Pt−X bond follows the order $Cl^- > NH_3$ (bpym) $> OSO_3H^- > \square$ (empty site). Thus the Pt−N bond length is longer and the Pt−N bond is weaker when the trans-influencing ligand is Cl^- than when it is OSO_3H^-.

All Pt complexes preserve the square-planar arrangement. The average Pt−X bond length follows the trend Pt−Cl (2.32 Å) > Pt−N (2.09 Å) > Pt−O (2.06 Å). ∠X−Pt−X bond angles are generally larger than ∠X−Pt−Y ($X \neq Y$) bond angles. In a T-complex, the length of a Pt−X bond (which is trans to ligand Y) is generally longer than that of the Pt−X bond, which is cis to ligand Y or trans to the empty site.

(3) As bpym is protonated, the Pt−N bond strength decreases instead of increases. ΔE(g, 0 K): $PtCl_2$(bpym) (87.0) > $[PtCl_2(bpymH)]^+$ (58.9) > $[PtCl_2(bpymH_2)]^{2+}$ (26.6); ΔH(s, 453 K): $PtCl_2$(bpym) (73.0) > $[PtCl_2(bpymH)]^+$ (60.0) > $[PtCl_2(bpymH_2)]^{2+}$ (38.5). This suggests its role as a σ-donor instead of being a π-acceptor as it is generally accepted.

(4) The Pt−Cl bond is stronger than the Pt−OSO_3H bond, making it easier to dissociate a Pt−OSO_3H bond.

(5) Since bpym is a weaker σ-donor than NH_3, bpym has a weaker trans-influence than NH_3. Thus it is easier to dissociate a Pt−Cl bond in $PtCl_2(NH_3)_2$ (ΔH(s, 453 K) = 23.8 kcal/mol) than to dissociate a Pt−Cl bond in $PtCl_2$(bpym) (ΔH(s, 453 K) = 36.0 kcal/mol).

(6) We find that replacement of ammine ligands with bisulfate ligands is thermodynamically favorable, while replacement of chloride ligands or bpym with bisulfate ligands is thermodynamically unfavorable. We find protonation of $PtCl_2$(bpym) is a thermodynamically favorable process.

(7) Our calculations show that $PtCl_2(NH_3)_2$ will lose its ammine ligands in hot concentrated sulfuric acid and that the $PtCl_2$ will dimerize and trimerize, leading to $(PtCl_2)_n$ precipitation. Our calculations show that $PtCl_2$(bpym) is indeed resistant to solvent attack, favorably retaining the bpym ligand in hot concentrated sulfuric acid, in agreement with the experimental findings.

(8) We find that both bisulfate forms, $[PtCl_2(OSO_3H)_2]^{2-}$ and $[PtCl_2(\eta^2\text{-}OSO_3H)]^-$, favorably form dimers and trimers. Protonated bpym catalysts, $[PtCl_2(bpymH_n)]^{n+}$ ($n = 0, 1, 2$), do not favor dimerization and trimerization. Although each Pt(II) keeps a local square-planar geometry, Pt(II) dimers and trimers adopt a bowl structure. A totally planar geometry does not correspond to a local minimum.

(9) Our calculations show that the affinity of bpym for Pt(II) is sufficiently high so that a treatment of bpym in hot, concentrated sulfuric acid will lead to the dissolution of insoluble $(PtCl_2)_n$ and the oxidative dissolution of Pt metal to make a homogeneous solution of the bpym catalyst, while no such dissolution occurs in the absence of the bpym ligand, in agreement with the experimental findings.

These findings should help the screening of new ligands for the design of new catalysts.

Appendix: Assessment of the Accuracy of the QM Calculations

Curtiss et al.[40] has reported that the B3LYP flavor of DFT using the 6-311+G(3df,2p) basis set leads to a mean average error (MAD) of 3.11 kcal/mol for heats of formation over the G2 set (a total of 148 molecules where accurate experimental data are available). Using the smaller 6-31G**+ basis set with Jaguar,[29] we obtain MAD = 5.1 kcal/mol for the G2 set. We would expect this to be the general accuracy for the gas phase reactions of the present study.

To assess the accuracy for solvation energy calculations for neutral organics, we considered the 55 neutral organic molecules with well established experimental data.[41] For B3LYP/6-31G**/PB using Jaguar,[29] we

(37) Barone V.; Cossi M.; Tomasi J. *J. Chem. Phys.* **1997**, *107*, 3210.
(38) Lide, D. R. *Handbook of Chemistry and Physics*, 82nd ed.; CRC Press: Boca Raton, FL, 2001−2002.
(39) Henry, P. M. *Palladium Catalyzed Oxidation of Hydrocarbons*; Reidel: Dordrecht, Netherlands, 1980.
(40) Curtiss, L. A.; Raghavachari, K.; Redfern P. C.; Pople, J. A. *J. Chem. Phys.* **1997**, *106*, 1063.
(41) Cabani S.; Molica G.; Lepori, V. *J. Sol. Chem.* **1981**, *10*, 563.

obtain MAD = 0.65 kcal/mol. This is likely within experimental error.

To assess the accuracy for solvation energy calculations of charged molecules, we considered 26 anions and cations (inorganics and organics) for which there are reviewed experimental data.[37] For B3LYP/6-31G**+/PB we find MAD = 5.4 kcal/mol. This is likely within experimental error since the experimental data for charged species are much less certain than for neutral species.

We may take reactions A1−A3 in aqueous solutions as examples to gauge the uncertainties associated with the present study.

$$NH_3 + H_2O \rightarrow NH_4^+ + OH^- \qquad (A1)$$

$$HSO_4^- + H_2O \rightarrow H_3O^+ + SO_4^{2-} \qquad (A2)$$

$$PtCl_2(c) + 2\ Cl^-(aq) \rightarrow PtCl_4^{2-}(aq) \qquad (A3)$$

Here pK_b of NH_3 and pK_a of H_2SO_4 can be related to the ability of NH_3 ligand to dissociate from $PtCl_2(NH_3)_2$ into solution as studied in the present work. Reaction A3 is $PtCl_2$(c) dissolution by coordination to Cl^- ligands, a process similar to $PtCl_2$(c) dissolution by bpym ligands studied in the present work.

Our calculated ΔG(s, 298 K) for reaction A1 is −6.6 kcal/mol, which can be compared to the experimental value of −6.5 kcal/mol.[38] Our calculated value for A2 is −3.1 kcal/mol, which can be compared to the experimental value of −2.6 kcal/mol.[38] This is amazingly good agreement, with errors smaller than the expected uncertainties in the DFT and solvation methods being employed.

We found no experimental data to directly estimate ΔG(s, 298 K) of reaction A3. However, we have estimated the experimental value as follows (based on numbers from the 2002 CRC handbook[38]).

From standard electrode potentials,

$$^1/_2\ PtCl_4^{2-}(aq) + e \rightarrow\ ^1/_2\ Pt(c) + 2\ Cl^-(aq) \qquad 0.758\ V \qquad (A4)$$

$$^1/_2\ Cl_2(g) + e \rightarrow Cl^-(aq) \qquad 1.3583\ V \qquad (A5)$$

we obtain

$$^1/_2\ PtCl_4^{2-}(aq) \rightarrow\ ^1/_2\ Pt(c) + {}^1/_2\ Cl_2(g) + 2\ Cl^-(aq) \qquad -0.6003\ V \qquad (A6)$$

Thus the reaction free energy change for reaction A6 is

$$\Delta G_r(\text{reaction A6}) = -23.06*(-0.6003) = 13.8\ \text{kcal/mol}$$

Taking account into that $\Delta G_f°(Cl^-, aq) = -31.4$, $\Delta G_f°(Cl_2, g) = 0$, and $\Delta G_f°(Pt, c) = 0$ kcal/mol,[38] we obtain $\Delta G_f°(PtCl_4^{2-}, aq) = -90.4$ kcal/mol.

We estimated the third law $\Delta S°$ for $PtCl_2$(c) according to the Latimer equation.[42] For two solid substances of similar formulas and similar melting points, the difference in entropy arises very largely from the mass effect. The knowledge of the entropy of one substance then permits a close estimate of the value for that of the other by the expression

$$\Delta S_A° - \Delta S_B° = 3/2\ R\ \ln([A]/[B])$$

Based on $\Delta S°(NiCl_2, c) = 23.4$ cal mol^{-1} K^{-1},[38] we obtain $\Delta S°(PtCl_2, c) = 27.0$. Thus $\Delta G_f°(PtCl_2, c)$ can be estimated using quantities in eq A7.

$$Pt(c) + Cl_2(g) \rightarrow PtCl_2(c) \qquad (A7)$$

Using $\Delta G_r = \Delta H_r - T\Delta S_r$, we arrive at $\Delta G_f°(PtCl_2, c) = -18.7$ kcal/mol.

$\Delta H_f°$	0.0	0.0	−29.5	$\Delta H_r = -29.5$ kcal/mol
$\Delta G_f°$	0.0	0.0	?	$\Delta G_r = \Delta G_f°(PtCl_2, c)$
$\Delta S°$	9.9	53.3	27.0	$\Delta S_r = -36.2$ cal mol^{-1} K^{-1}

In this way, we obtain that the reaction free energy change of reaction A3 is

$$\Delta G_r(\text{reaction A3}) = -9.1\ \text{kcal/mol}$$

based on $\Delta G_f°(PtCl_4^{2-}, aq) = -90.4$, $\Delta G_f°(Cl^-, aq) = -31.3$, and $\Delta G_f°(PtCl_2, c) = -18.7$ kcal/mol.

Generally cluster models are not expected to give directly accurate cohesive energies for bulk solids. However we find the following based on B3LYP/LACVP**(+)/PB:

reaction	ΔG(s,298K)/kcal/mol
$PtCl_2 + 2\ Cl^- \rightarrow PtCl_4^{2-}$	−28.9
$1/2\ (PtCl_2)_2 + 2\ Cl^- \rightarrow PtCl_4^{2-}$	−19.0
$1/3\ (PtCl_2)_3 + 2\ Cl^- \rightarrow PtCl_4^{2-}$	−21.9
$1/6\ (PtCl_2)_6 + 2\ Cl^- \rightarrow PtCl_4^{2-}$	−12.2

Here we have assumed that the bulk solid $PtCl_2$(c) has a crystal structure[43] consisting of hexamer Pt_6Cl_{12} molecules (although some have suggested that it adopts a chain structure[43]). Our result of −12.2 kcal/mol compares well with our estimated experimental result (−9.1 kcal/mol) for reaction A3.

Finally, we emphasize the importance of doing systematic studies, as above. The trends obtained by comparing all available data should be more reliable than a single number of a specific reaction. This is especially important when experimental data are sparse.

Acknowledgment. This research was initiated with funding from BP and the NSF (CHE 95-22179) and completed with funding from Chevron. We thank Dr. Bill Schinski, Dr. Rick Muller, Dr. Yongchun Tang, and Dr. Dean Philipp for helpful suggestions. The facilities of the MSC are also supported by grants from DOE-ASCI, ARO/DURIP, ARO/MURI, NIH, NSF (CTS-0132002, CHE-9985474), Beckman Institute, Seiko-Epson, 3M, Avery-Dennison, Dow, Kellogg's, and Asahi Chemical.

OM0202165

(42) Latimer, W. M. *The Oxidation States of the Elements and Their Potentials in Aqueous Solution*; Printice Hall: New Jersey, 1952.

(43) Wells, A. F. *Structural Inorganic Chemistry*, 5th ed.; Oxford, 1984.